WATER RESOURCES RESEARCH, VOL. 47, W02505, doi:10.1029/2010WR009608, 2011

Transverse mixing of conservative and reactive tracers in porous media: Quantification through the concepts of flux-related and critical dilution indices

Gabriele Chiogna,[1] Olaf A. Cirpka,[1] Peter Grathwohl,[1] and Massimo Rolle[1]

Received 2 June 2010; revised 30 September 2010; accepted 2 November 2010; published 3 February 2011

[1] The correct quantification of mixing is of utmost importance for modeling reactive transport in porous media and for assessing the fate and transport of contaminants in the subsurface. An appropriate measure of mixing in heterogeneous porous formations should correctly capture the effects on mixing intensity of various processes at different scales, such as local dispersion and the mixing enhancement due to heterogeneities. In this work, we use the concept of flux-related dilution index as a measure of transverse mixing. This quantity expresses the dilution of the mass flux of a conservative tracer solution over the total discharge of the system, and is particularly suited to address problems where a compound is continuously injected into the domain. We focus our attention on two-dimensional systems under steady state flow conditions and investigate both conservative and reactive transport in homogeneous and heterogeneous porous media at different scales. For mixing-controlled reactive systems, we introduce and illustrate the concept of critical dilution index, which represents the amount of mixing required for complete degradation of a continuously emitted plume undergoing decay upon mixing with ambient water. We perform two-dimensional numerical experiments at bench and field scales in homogeneous and heterogeneous conductivity fields. These numerical simulations show that the flux-related dilution index quantifies mixing and that the concept of critical dilution index is a useful measure to relate the mixing of conservative tracers to mixing-controlled degradation of reactive compounds.

Citation: Chiogna, G., O. A. Cirpka, P. Grathwohl, and M. Rolle (2011), Transverse mixing of conservative and reactive tracers in porous media: Quantification through the concepts of flux-related and critical dilution indices, *Water Resour. Res., 47*, W02505, doi:10.1029/2010WR009608.

1. Introduction

[2] A detailed characterization of mixing in geologic formations and fixed-bed reactors is relevant in order to correctly quantify and describe reactive processes in porous media. In particular, many biodegradation reactions may be limited by the availability of reaction partners. Under steady state flow and transport conditions, dissolved reactants come into contact through transverse mixing, which is determined by dilution processes in the directions perpendicular to flow (i.e., processes which increase the entropy and decrease the peak concentration of conservative solutes). In particular, we consider steady state two-dimensional transport of two reacting species continuously injected in parallel. In homogenous media, transverse mixing is determined by molecular diffusion and dispersion, while in heterogeneous formations, this local mixing process is enhanced by flow focusing within high-permeability inclusions [*Bear*, 1972; *Kitanidis*, 1994; *Werth et al.*, 2006; *Rolle et al.*, 2009]. The Darcy-scale processes can be investigated through laboratory experiments and are typically modeled by Fickian dispersion. Although different theories and empirical expressions were proposed to compute the components of the local dispersion tensor [e.g., *Scheidegger*, 1961; *Bear*, 1972; *Klenk and Grathwohl*, 2002], a general agreement exists about the order of magnitude of these parameters.

[3] The enhancement of transverse mixing due to the presence of advective heterogeneities is more difficult to quantify. The focusing of streamlines in high-conductivity zones is known to be one of the mechanisms that enhance transverse mixing since it reduces the transverse mixing length, increasing the mass flux across streamlines [*Werth et al.*, 2006, *Rolle et al.*, 2009]. However, a quantitative parameter to capture this effect would require field-scale experiments in which the heterogeneities are very well characterized; such experiments are, unfortunately, not feasible, and usually, the details of the flow field remain widely unknown. Furthermore, the presence of heterogeneities may stretch and squeeze the plume and lead to meandering [e.g., *Rahman et al.*, 2005]. However, as pointed out by *Kitanidis* [1994], these processes do not directly contribute to physical mixing. Squeezing and stretching are mass displacements connected with advection mechanisms, and hence, they are not strictly mixing or demixing processes, even if

---

[1] Center for Applied Geoscience, University of Tübingen, Tübingen, Germany.

Copyright 2011 by the American Geophysical Union.
0043-1397/11/2010WR009608

they affect the second central transverse moments of the plume [*Rahman et al*., 2005; *Rolle et al*., 2009]. Meandering causes an increase in the uncertainty of the plume's first transverse moment but does not contribute to a net increase in transverse mixing. Stochastic analysis has dealt mainly with ensemble behavior of spatial moments in order to quantify dispersion in heterogeneous formations. Half the rate of change of second central moments of the ensemble concentration defines the ensemble dispersion tensor [*Gelhar and Axness*, 1983; *Dagan*, 1984; *Neuman et al*., 1987], which does not quantify mixing properly; in fact, it is still affected by the uncertainty of tagging the plume center (i.e., it is affected by meandering). Although commonly used, ensemble dispersion is not a measure of pure mixing. Another possibility is to define so-called effective dispersion. The conceptual model underlying the effective dispersion tensor differs from ensemble dispersion in the order of taking spatial moments and averaging over all realizations. In effective dispersion, the second central moments of each realization are evaluated first, and the ensemble average of the second central moments is obtained subsequently [*Kitanidis*, 1988; *Dagan*, 1990, 1991; *Rajaram and Gelhar*, 1993a, 1993b, 1995; *Dentz et al*., 2000a]. It is possible to define effective transverse dispersion coefficients for wide plumes [e.g., *Dentz et al*., 2000b]. In this case both the irregular plume shape and the smooth transition of concentration from the plume center to the surrounding area are quantified. Only the latter property is related to actual mixing of the plume with ambient water, while the former quantifies an average squeezing and stretching. Effective transverse dispersion coefficients can also be defined for point-like injections [*Dentz et al*., 2000a; *Cirpka*, 2002; *Dentz and Carrera*, 2003, 2005]. As claimed by *Cirpka* [2002], this is a good measure of mixing for reactive transport in case of complete mixing at the Darcy scale [*Tartakovsky et al*., 2009] since the scale of chemical transformation is the local one and in this way it is possible to quantify mixing. Unfortunately, this measure is not applicable to individual plumes; it is not a measure for plumes of finite width, and it is affected by very high uncertainty. The mentioned stochastic approaches consider expected ensemble behavior and cannot cover the uncertainty of mixing and thus the variability of observable mixing in real measurements.

[4] In multispecies (bio)reactive transport [e.g., *Cirpka and Valocchi*, 2007; *Prommer et al*., 2009], the limiting step for the reaction is the mixing between the different reactive compounds, if this process is slower than the (bio)-chemical reaction. At steady state, the reaction partners must be mixed into the plume from the sides, hence the most important components of the dispersion tensor are the transverse ones [*Cirpka et al*., 1999a; *Liedl et al*., 2005]. The mixing processes of real interest are the ones at the pore scale [*Willingham et al*., 2008, 2010] since reactions occur at a narrow reactive fringe, as shown by field-scale measurements [*Lerner et al*., 2000; *Anneser et al*., 2008] as well as by laboratory bench-scale experiments [*Bauer et al*., 2009]. In order to estimate the length of a reactive plume in heterogeneous flow fields, we have to estimate the effect of advective heterogeneities and, in particular, of flow focusing on the enhancement of mixing and reaction [*Werth et al*., 2006; *Rolle et al*., 2009]. Hence, we have to consider a process at a larger scale than the pore one.

[5] *Kitanidis* [1994] proposed to quantify mixing processes in groundwater by measuring the entropy of the plume, introducing the concept of the dilution index. This kind of measurement was applied to determine mixing of conservative tracers at the laboratory [e.g., *Ursino et al*., 2001; *Moroni et al.,* 2007; *Rossi et al*., 2007, 2008] and at the field scale [e.g., *Thierrin and Kitanidis*, 1994]. The dilution index was also used in pore-scale modeling [e.g., *Cao and Kitanidis*, 1998], in modeling studies in heterogeneous porous media [*Kapoor and Kitanidis*, 1996, 1998; *Beckie*, 1998; *Pannone and Kitanidis*, 1999; *McLaughlin and Ruan*, 2001], and even to determine numerical dispersion of transport codes [*Chilakapati and Yabusaki*, 1999]. Recently, this measure was applied in pore-scale multicomponent reactive transport simulations [*Tartakovsky et al*., 2009]. The dilution index was modified by *de Rooij et al*. [2006] to apply it to breakthrough curves obtained by multicompartment sampler data and later used by *Bloem et al*. [2009] for the interpretation of field experiments. *Bear and Sun* [1998] slightly modified the dilution index in order to account for changes in the porosity of the system, which was assumed constant by *Kitanidis* [1994].

[6] The dilution index as implemented by *Kitanidis* [1994] is a useful measure in case of a slug injection, while for continuous injections a flux-related dilution index appears to be more appropriate [*Rolle et al*., 2009]. In this work we further develop the concept of flux-related dilution index, providing analytical expressions to compute its value in homogeneous porous media and comparing it with the volumetric dilution index presented by *Kitanidis* [1994] (section 2). More importantly, we focus our attention on the reactive case (section 3): We define the effective transverse dispersion coefficient needed in an equivalent homogeneous system to match the reactive behavior in a heterogeneous one, and we relate it to the dilution of a conservative tracer. This is accomplished through the introduction of the critical dilution index. This parameter quantifies the degree of mass flux dilution required to obtain complete degradation of a reactive plume emitted from a continuous line source. In section 4, we present the results of numerical simulations of laboratory bench-scale systems and larger binary heterogeneous flow fields to show the applicability of the flux-related and critical dilution indices.

2. Flux-Related Dilution Index for Conservative Transport

[7] The flux-related dilution index E_Q [$L^3\ T^{-1}$], introduced by *Rolle et al.* [2009], describes dilution "as the act of distributing a given solute mass flux over a larger water flux" (p. 136) and quantifies how the continuous mass flux of a conservative compound is mixed in a given flow field. The concentrations considered are local flux concentrations (i.e., the solute mass flux perpendicular to the control plane, divided by the specific discharge in the same direction), which differ slightly from the resident concentrations [*Kreft and Zuber*, 1978]. In contrast, the original dilution index of *Kitanidis* [1994] considered dilution as "the act of distributing (a finite slug of) solute mass over a larger volume." (p. 2015) The possibility to work with mass fluxes, instead of a finite mass, allows investigating how the dilution of a solute flux increases with travel distance when the

compound is continuously injected into the flow domain. An ad hoc transfer of the original dilution index to the situation of a continuously emitting source would be to consider the distribution of solute mass over a larger cross-sectional area perpendicular to the mean direction of flow. Such a concept would fail in the presence of heterogeneities where the cross-sectional area of a plume may shrink and expand due to spatially variable advection alone. In fact, as derived in Appendix A, weighting the dilution index with the flow velocity is necessary to obtain a measure of mixing [*Rolle et al.*, 2009; *Chiogna et al.*, 2010a]. Both formulations of the dilution index intend to quantify mixing by the exponent of the entropy of the system. Entropy in this case has to be interpreted as a local spatial measure of dilution and not as a thermodynamic quantity [*Beckie*, 1998]. In Table 1, we compare the distribution functions and the different definitions of the volumetric and flux-related dilution indices and of the reactor ratios (the normalized version of the dilution indices for a bounded domain). We also compare the rate of increase of the dilution index with time and of the flux-related dilution index with distance; the derivation of the latter is summarized in Appendix A. The concentration of the tracer solution is expressed by c $[M\,L^{-3}]$, the cross-sectional area by A $[L^2]$, the volume by V $[L^3]$, the porosity by n (dimensionless), the specific-discharge component in the x direction by q_x $[L\,T^{-1}]$, and the total discharge by Q_x $[L^3\,T^{-1}]$. We assume that the flow is generally oriented in the x direction and that q_x is positive throughout the domain (i.e., we do not consider cases in which strong heterogeneity contrasts may cause a local flow reversal).

[8] The volumetric dilution index introduced by *Kitanidis* [1994] is a function of time, while the flux-related dilution index of *Rolle et al.* [2009] is a function of space. It can be noticed that the rate of increase of both indices is the same, with the important difference that for the first one we consider the time derivative, while for the second one we consider the spatial derivative in the flow direction. The rate of increase of the entropy depends critically on the shape of the plume and on its interfacial area [*Kitanidis*, 1994] in both concepts. The property of being a monotonic increasing function is a necessary condition for both formulations of the dilution index. This allows us to capture the essential characteristics of dilution processes which are irreversible and lead to a continuous increase of the entropy of the plume in both homogeneous and heterogeneous flow fields.

[9] The volumetric expression for the dilution index can be restricted to a cross-sectional dilution index E_{cs} $[L^2]$, obtained by considering only the transverse coordinates (i.e., we integrate the entropy over a cross section of the domain instead over the whole volume; see Appendix B). At steady state in a homogeneous domain, the interpretation of the flux-related dilution index is strongly related to the cross-sectional dilution index and therefore to the original volumetric expression introduced by *Kitanidis* [1994]. In this context, we may transfer the longitudinal coordinate x of the cross section to the equivalent travel time x/v. Then, the flux-related dilution index in a uniform medium scales linearly with the cross-sectional dilution index by a factor of q_x (Appendix B):

$$\frac{E_Q(x)}{q_x(\mathbf{x})} = E_{\mathrm{cs}}(x). \qquad (1)$$

[10] For a line source of width w [L] in the y direction in an unbounded two-dimensional domain at steady state, we can express the flux-related dilution index as a function of the inverse transverse Péclet number (ε_y), defined as

$$\varepsilon_y = \frac{nxD_t}{q_x w^2}, \qquad (2)$$

where n [-] is the porosity of the system, D_t $[L^2\,T^{-1}]$ is the local transverse dispersion coefficient, and the flow is oriented in the x direction.

[11] For this geometry, we obtain the following expression of $E_Q(\varepsilon_y)$ (Appendix C):

$$E_Q(\varepsilon_y) = wZq_x\left(1 - \sqrt{\frac{4\pi\varepsilon_y}{4\pi\varepsilon_y + 1}} + \sqrt{4\pi\exp(1)\varepsilon_y}\right), \qquad (3)$$

where Z $[L]$ is the thickness of the system in direction z.

[12] This analytical expression (equation (3)) is in very good agreement with the result obtained from a numerical computation of the flux-related dilution index for a line source in a 2-D unbounded homogeneous domain (Figure 1).

[13] In Appendix C, we briefly illustrate other analytical expressions of the flux-related dilution index for different homogeneous flow domains (with the flow oriented in the x direction) and boundary conditions.

Table 1. Definition and Properties of the Volumetric Dilution Index $E(t)$ and the Flux-Related Dilution Index $E_Q(x)$

	Volumetric Dilution Index[a]	Flux-Related Dilution Index[b]
Density function	$p(\mathbf{x},t) = \frac{c(\mathbf{x},t)}{\int_V c(\mathbf{x},t)\mathrm{d}V}\left[\frac{1}{L^3}\right]$ $\int_V p(\mathbf{x},t)\mathrm{d}V = 1$	$p_Q(\mathbf{x}) = \frac{c(\mathbf{x})}{\int_A q_x(\mathbf{x})\cdot c(\mathbf{x})\mathrm{d}y\mathrm{d}z}\left[\frac{T}{L^3}\right]$ $\int_A p_Q(\mathbf{x})q_x(\mathbf{x})\mathrm{d}y\mathrm{d}z = 1$
Dilution index	$E(t) = \exp\left\{-\int_V p(\mathbf{x},t)\ln[p(\mathbf{x},t)]\mathrm{d}V\right\}[L^3]$	$E_Q(x) = \exp\left\{-\int_A p_Q(\mathbf{x})\ln\left[p_Q(\mathbf{x})\right]\cdot q_x(\mathbf{x})\mathrm{d}y\mathrm{d}z\right\}\left[\frac{L^3}{T}\right]$
Reactor ratio	$M(t) = \frac{E(t)}{V}$	$M_Q(x) = \frac{E_Q(x)}{Q_x}$
Rate of increase	$\frac{\mathrm{d}\ln(E)}{\mathrm{d}t} = -\int_V p\nabla\ln p^T\mathbf{D}\nabla\ln p\mathrm{d}V\left[\frac{1}{T}\right]$	$\frac{\mathrm{d}\ln(E_Q)}{\mathrm{d}x} = -\int_A p_Q\nabla\ln p_Q{}^T\mathbf{D}\nabla\ln p_Q\mathrm{d}y\mathrm{d}z\left[\frac{1}{L}\right]$

[a] *Kitanidis* [1994].
[b] *Rolle et al.* [2009].

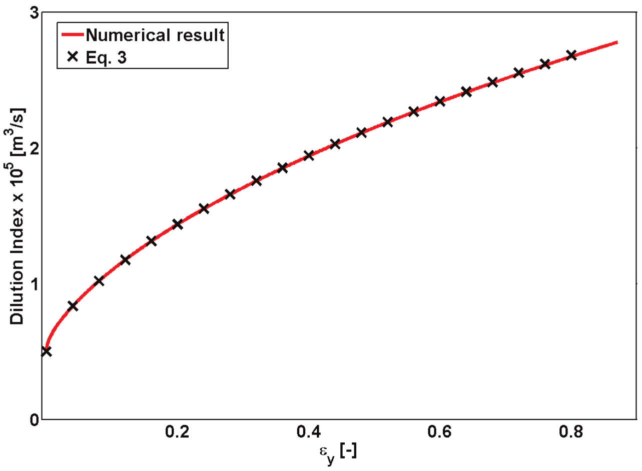

Figure 1. Comparison between the values of the dilution index computed numerically and analytically (equation (3)) for a line source in a 2-D unbounded homogeneous domain.

3. Critical Dilution Index for Reactive Transport

3.1. Reactive Transport Problem

[14] For simplicity, we restrict our analysis to conservative and reactive transport in a two-dimensional domain under steady state conditions. We assume an instantaneous bimolecular complete reaction of the form $aA + bB \rightarrow cC$ (where a, b, and c are the stoichiometric coefficients) so that the reaction rate is controlled only by the mixing process between the species A and B. The reacting compound A is injected through a continuous line source at the inflow boundary, while B is introduced from its sides into the domain with the ambient groundwater. Figure 2 shows two examples of the heterogeneous flow fields at different scales considered in this work. The continuous line source of compound A is highlighted on the left boundary of the domain.

[15] Assuming that aqueous diffusion coefficients are identical for all reactive species, we can simplify the problem by considering a virtual conservative compound X, denoted as the mixing ratio of the plume [*De Simoni et al.*, 2005, 2007; *Cirpka and Valocchi*, 2007], introduced with unit concentration through the line source:

$$\begin{aligned} &\mathbf{v}\cdot\nabla X - \nabla\cdot(\mathbf{D}\nabla X) = 0, \\ &\mathbf{n}\cdot(\mathbf{v}X - \mathbf{D}\nabla X) = \mathbf{n}\cdot\mathbf{v} \quad \text{along } \Gamma_{\mathrm{in}}^{\mathrm{A}}, \\ &\mathbf{n}\cdot(\mathbf{v}X - \mathbf{D}\nabla X) = 0 \quad \text{along } \Gamma_{\mathrm{in}}^{\mathrm{B}}, \\ &\mathbf{n}\cdot\mathbf{D}\nabla X = 0 \quad \text{along } \Gamma_{\mathrm{nf}}\cup\Gamma_{\mathrm{out}}, \end{aligned} \tag{4}$$

where the seepage velocity $\mathbf{v}$ is mainly oriented in the x direction and is expressed as $v = qn^{-1}$ [$L\ T^{-1}$] (for simplicity, hereafter we will leave the subscription x), $\Gamma_{\mathrm{in}}{}^{\mathrm{A}}$ and $\Gamma_{\mathrm{in}}{}^{\mathrm{B}}$ are the fractions of the inflow boundary where compounds A and B are introduced, respectively, Γ_{nf} is a no-flow boundary, and Γ_{out} is the outflow boundary. The local transverse dispersion coefficient D_t is defined following the

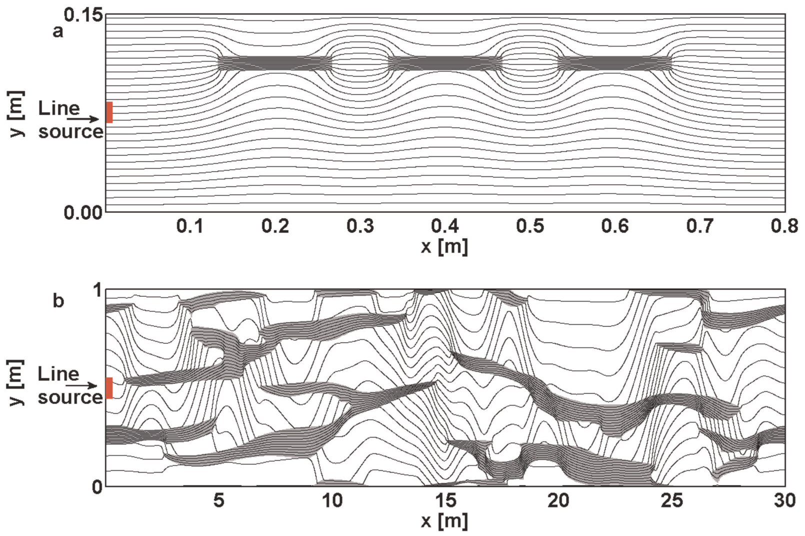

Figure 2. Streamlines computed for (a) a bench-scale and (b) a field-scale binary heterogeneous porous media. The gray zones where the streamlines converge are the high-conductivity inclusions.

nonlinear empirical parameterization recently proposed by *Chiogna et al.* [2010b]:

$$D_t = D_p + \frac{vd}{\sqrt{Pe + 123}}, \tag{5}$$

where D_p [$L^2\ T^{-1}$] is the pore diffusion coefficient, i.e., the ratio between the aqueous diffusion coefficient D_{aq} [$L^2\ T^{-1}$] and the tortuosity factor of the porous medium τ ([-]; in this work we assume $\tau = n^{-1}$), d [L] is the grain size diameter, and $Pe = vd/D_{\mathrm{aq}}$ [-] is the grain Péclet number.

[16] The mixing ratio can be converted to concentrations of reactive compounds by [*Cirpka and Valocchi*, 2007]

$$\begin{aligned}
C_{\mathrm{A}} &= \begin{cases} XC_{\mathrm{A}}^{\mathrm{in}} - \frac{a}{b}(1-X)C_{\mathrm{B}}^{\mathrm{amb}} & \mathrm{if} X \geq X_{\mathrm{crit}} \\ 0 & \mathrm{if} X < X_{\mathrm{crit}} \end{cases}, \\
C_{\mathrm{B}} &= \begin{cases} (1-X)C_{\mathrm{B}}^{\mathrm{amb}} - \frac{b}{a}XC_{\mathrm{A}}^{\mathrm{in}} & \mathrm{if} X < X_{\mathrm{crit}} \\ 0 & \mathrm{if} X \geq X_{\mathrm{crit}} \end{cases}, \\
C_{\mathrm{C}} &= \begin{cases} \frac{c}{a}XC_{\mathrm{A}}^{\mathrm{in}} & \mathrm{if} X < X_{\mathrm{crit}} \\ \frac{c}{b}(1-X)C_{\mathrm{B}}^{\mathrm{amb}} & \mathrm{if} X \geq X_{\mathrm{crit}} \end{cases},
\end{aligned} \tag{6}$$

in which $C_{\mathrm{A}}^{\mathrm{in}}[M\,L^{-3}]$ and $C_{\mathrm{B}}^{\mathrm{amb}}[M\,L^{-3}]$ are the inlet concentration of compound *A* and the inlet (and ambient) concentration of compound *B*, respectively, and X_{crit} is the critical mixing ratio at which both reactive species concentrations are zero:

$$X_{\mathrm{crit}} = \frac{aC_{\mathrm{B}}^{\mathrm{amb}}}{aC_{\mathrm{B}}^{\mathrm{amb}} + bC_{\mathrm{A}}^{\mathrm{in}}}. \tag{7}$$

[17] For the homogeneous case with the source width *w* [*L*], *X* will satisfy the two-dimensional analytical solution for the transport of a conservative species continuously injected by a line source [*Domenico and Palciauskas*, 1982]:

$$X(x,y) = \frac{1}{2}\left[\mathrm{erf}\left(\frac{y + \frac{w}{2}}{2\sqrt{D_t \frac{x}{v}}}\right) - \mathrm{erf}\left(\frac{y - \frac{w}{2}}{2\sqrt{D_t \frac{x}{v}}}\right)\right]. \tag{8}$$

[18] As pointed out by *Srinivasan et al.* [2007], this approximate analytical solution is subject to some limiting constraints. In this work we assume that those constraints are met, and we rely on the applicability of equation (8).

3.2. Definition and Derivation of the Critical Dilution Index

[19] In section 2, we have defined the flux-related dilution index, which measures the degree of dilution of a continuously emitted conservative tracer undergoing steady state transport. We can now try to answer the following questions: (1) How are the dilution of a conservative and a reactive compound related? (2) Which information can be extrapolated from a conservative plume to a reactive plume? (3) How much mixing is required to achieve the complete degradation of a reactive plume?

[20] The plume length of the injected compound *A* is defined as the minimal distance *L* [*L*] from the source in the average flow direction at which $C_{\mathrm{A}} = 0$ over the entire cross-sectional profile perpendicular to the average flow direction [*Cirpka et al.*, 2006]. The mixing ratio exactly has the value $X = X_{\mathrm{crit}}$, where the concentration of both *A* and *B* are zero. For the homogeneous case and when equation (8) is valid, we obtain [*Cirpka et al.*, 2006]

$$L = \frac{vw^2}{16D_t \mathrm{inverf}(X_{\mathrm{crit}})^2}. \tag{9}$$

[21] In the case of an instantaneous reaction (i.e., the reaction occurs immediately upon mixing), the boundary of the plume is defined by $X = X_{\mathrm{crit}}$, stemming from the stoichiometry of the reaction, the inflow, and ambient concentrations. This distance of the farthest downstream point with $X = X_{\mathrm{crit}}$ (i.e., the plume length) depends on hydraulic parameters (e.g., dispersion coefficient and heterogeneity), but the required amount of mixing between *A* and *B* will be similar for any hydraulic setting.

[22] We now define the critical dilution index as the amount of mixing required for complete degradation of a reactive compound that is continuously injected into a porous medium and reacts with another compound injected in parallel. We hypothesize that the required amount of mixing is unique (or at least affected by a negligible variance) when the aqueous diffusion coefficients (and hence the transverse dispersion coefficients) of the different reaction partners are the same. We define the critical dilution index as the value of the flux-related dilution index of a given conservative tracer at the length *L* of the reactive plume in the same flow field and for the same mass flux. For the homogeneous case, it is possible to demonstrate analytically that the value of the critical dilution index depends on the mass flux of the solute and on the critical mixing ratio (Appendix D).

[23] Figure 3 shows the plume of a conservative compound in a homogeneous flow field: the white contour represents the normalized concentration $C(x,y)/C_0 = X_{\mathrm{crit}}$, i.e., the boundary of a reactive plume. It is worth noting that the $C(x,y)/C_0$ profile at a cross section before the end of reactive plume exhibits the value of X_{crit} at two locations and the reactive plume extends farther into the domain (Figure 3, bottom, profile A). At a cross section beyond the end of the reactive plume, the concentration ratio never reaches the value of X_{crit} (i.e., the reactive plume never reaches that distance). At the distance where the reactive plume ends, the transverse normalized concentration value $C(L,y)/C_0$ has the critical mixing ratio X_{crit} as its maximum (Figure 3, bottom, profile B). This behavior also holds for heterogeneous cases. At steady state, the maximum of the normalized concentration of a conservative compound (i.e., the mixing ratio) will always be a continuously decreasing function with distance, and the length of a reactive plume is uniquely related to a particular maximum, corresponding to the critical mixing ratio (X_{crit}). Quite obviously, since the total mass flux of the conservative compound does not change with distance, a decrease of the maximum concentration requires the distribution over a larger water flux, that is, dilution. We hypothesize that the relationship between the degree of dilution and the maximum

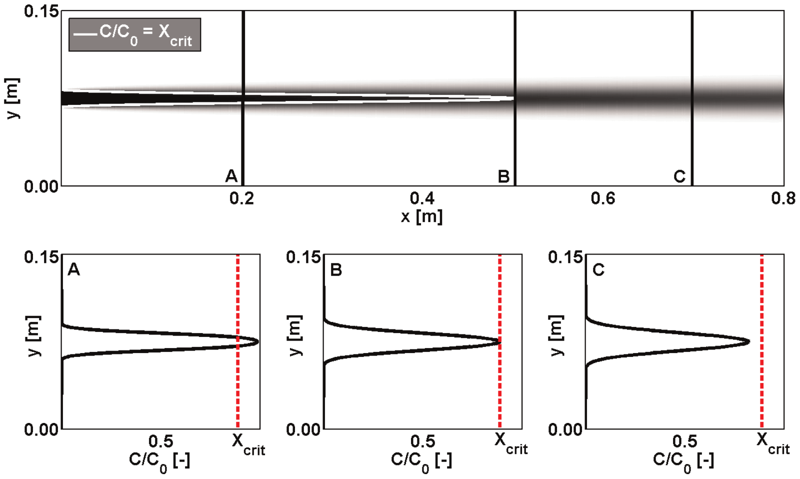

Figure 3. (top) Conservative plume in a homogenous bench-scale domain. The critical mixing ratio X_{crit} determines the boundary of the reactive plume (white contour line). (bottom) The vertical profiles of the normalized concentration of the conservative plume compared with the critical mixing ratio at different cross sections (i.e., 0.2, 0.5, and 0.7 m in profiles A, B, and C, respectively).

concentration does not vary significantly with the specific flow field.

[24] Considering a continuous injection through a line source under steady state flow conditions, we obtain for the critical dilution index (CDI), as a first order approximation,

$$\mathrm{CDI} = E_Q(L) = \frac{E_Q(0)}{X_{\text{crit}}}\exp(1/2). \tag{10}$$

[25] As discussed in Appendix C, equation (10) applies under the assumptions of validity of the analytical solutions (8) and (9).

[26] No analytical solution is available to predict the concentration distribution in heterogeneous flow fields. However, in order to directly compare the critical dilution index of the homogeneous porous media (equation (10)) with any heterogeneous setup we construct an equivalent homogeneous system. We define this system as the equivalent homogenous domain characterized by (1) the same injected solute mass flux as in the heterogeneous case and (2) an effective transverse dispersion coefficient leading to the same reactive plume length as in the heterogeneous domain. Using equation (9) and assuming we know the plume length of the heterogeneous case, the effective transverse dispersion coefficient of the equivalent homogeneous system will be

$$D_{t,\text{eff}} = \frac{vw^2}{16L\,\mathrm{inverf}(X_{\text{crit}})^2}. \tag{11}$$

[27] This definition of the effective dispersion coefficient differs from that proposed by *Kitanidis* [1988] and *Dentz et al.* [2000a], which relates to spatial moments of the plume. We have to point out that the effective transverse dispersion coefficient of the equivalent system will usually be larger than the mean local transverse dispersion coefficient because it includes effects of heterogeneity on mixing, but it does not quantify the spreading, the stretching, and the meandering of the plume in the heterogeneous case. By construction, at distance L the equivalent homogeneous system will exhibit a maximum of X equal to the critical value X_{crit}. We expect, in general, that in a spatially variable permeability field the degree of mixing will be different than in a homogeneous one. However, at the end of the reactive plume, according to the results of *Valocchi et al.* [2009], we hypothesize that the dilution undergone by a conservative tracer is very similar for the homogeneous and any heterogeneous cases. In fact, given the same mass flux and inflow concentrations at the boundary, we expect to obtain values for the critical dilution index very close to each other, independently from the heterogeneity of the system. Hence, as long as the flux-related dilution index does not reach the critical dilution index value, the plume will propagate farther both into the heterogeneous and into the homogeneous domains.

[28] The concept of critical dilution index establishes a relationship between the dilution of a conservative tracer and the behavior of a compound undergoing a reaction. Furthermore, it quantifies, for a given mass flux and a given reaction stoichiometry, to which extent a reactive species should be mixed with ambient water in order to be completely degraded. The advantage of the critical dilution index is that it connects a well-known physical quantity, i.e., the entropy generated by mixing, with the possibility to predict at which distance a reactive plume will be completely degraded.

4. Transport Simulations at Different Scales

[29] We perform two kinds of numerical experiments: in the first one, two-dimensional laboratory bench-scale experiments [e.g., *Bauer et al.,* 2009; *Rolle et al.*, 2009, 2010] are simulated both under homogeneous and heterogeneous conditions; in the second one, we perform two-dimensional field-scale simulations in heterogeneous systems. The

Table 2. Model Parameters

Parameter	Value
Bench-scale domain dimension (m)	$0.8 \times 0.01 \times 0.13$ ($L \times W \times H$)
Field-scale domain dimension (m)	$30 \times 1 \times 1$ ($L \times W \times H$)
Tortuosity factor	2.5
d coarse sand (m)	0.78×10^{-3}
d fine sand (m)	0.25×10^{-3}
K coarse sand (m s^{-1})	6.14×10^{-3}
Discretization (cells)	$600 \times 1 \times 1000$
Stoichiometric coefficients $a = b = c$	1
D_{aq} (m^{2}s^{-1})	0.8×10^{-9}
Field-scale specific discharge (m^{3}s^{-1})	5×10^{-5}
Bench-scale specific discharge (m^{3}s^{-1})	0.75×10^{-5}
K fine sand (m s^{-1})	6.14×10^{-4}

parameters of the numerical examples are summarized in Table 2.

[30] In the heterogeneous bench-scale experiment, three high-permeability inclusions (each 0.14 m long and 0.01 m wide) are placed at a distance of 0.13, 0.33, and 0.53 m from the inflow boundary. Ten cases are considered, each one differing from the previous one by shifting the lenses 0.01 m upward, the first one being aligned with the centerline of the tank. In the field-scale simulations, the heterogeneities are stochastically generated: irregularly shaped high-permeability inclusions are created using an auxiliary normal distributed variable with zero mean, Gaussian covariance function, longitudinal correlation length of 2 m, and lateral correlation length of 0.1 m, as described by *Werth et al.* [2006]. In order to simulate naturally occurring inclusions where the bottom surfaces are more curved than the top surfaces, a cutoff value for the auxiliary variable is set to represent the 40% quantile, and as a further constraint its vertical gradient component must be positive in the elements belonging to a high-conductivity lens. In both the field- and bench-scale simulations, the heterogeneous field is binary, the system is confined, fixed head boundary conditions are applied at the left- and right-hand-side boundaries, and the mass flux of the injected solution is identical in all realizations. Heterogeneities thus lead to variations of the source width between the realizations, but we can define an effective source width by the width in an equivalent homogeneous medium [*de Barros and Nowak*, 2010].

[31] The steady state flow problem for hydraulic head h and stream function ψ

$$
\begin{aligned}
&-\nabla \cdot (K \nabla h) = 0 \\
&-\nabla \cdot \left(\frac{1}{K} \nabla \psi \right) = 0
\end{aligned}
\tag{12}
$$

is computed on a rectangular mesh grid by finite elements.

[32] For the transport problem (equation (4)), the domain is discretized into 600 × 1000 finite volumes with streamline-oriented cells constructed by the approach of *Cirpka et al.* [1999b, 1999c]. The discharge is identical in all stream tubes. Figure 2 illustrates that streamlines are focused in inclusions of high-conductivity (light gray), leading to narrow elongated cells in that region. Orienting the grid in the flow direction avoids numerical transverse dispersion caused by diagonal fluxes between the cells; hence, no artificial mixing entropy is generated through numerical errors. The transport problem is solved using the UMFPACK direct solver of Matlab© [*Davis and Duff*, 1997]. Since we work under the assumption that all species are characterized by the same aqueous diffusion coefficient, we can use the postprocessing procedure of *Cirpka and Valocchi* [2007] in order to evaluate the reactive concentration values for compounds A, B, and C (equation (7)) from the mixing ratio X. The ambient concentration of compound B is kept constant, i.e., $C_B^{amb} = 1$, while the inlet concentration C_A^{in} of compound A is varied in order to obtain different values for X_{crit}. The stoichiometric coefficients a, b, and c are set to unity.

4.1. Results of Conservative Transport Simulations

[33] Figure 4 shows simulated plumes for different homogeneous and heterogeneous porous media at the bench scale. The behavior of the flux-related reactor ratio (M_Q) in a homogeneous setup is compared with the results of three heterogeneous cases. In the first heterogeneous domain (Figure 4, HET A), in which the plume is focused in the high-conductivity inclusions, the concentration is distributed over a larger water flux, and hence, the value of M_Q shows a steep increase (i.e., the increase in dilution leads to an effective mixing enhancement). The high-conductivity zones are almost in line with the source so that the whole

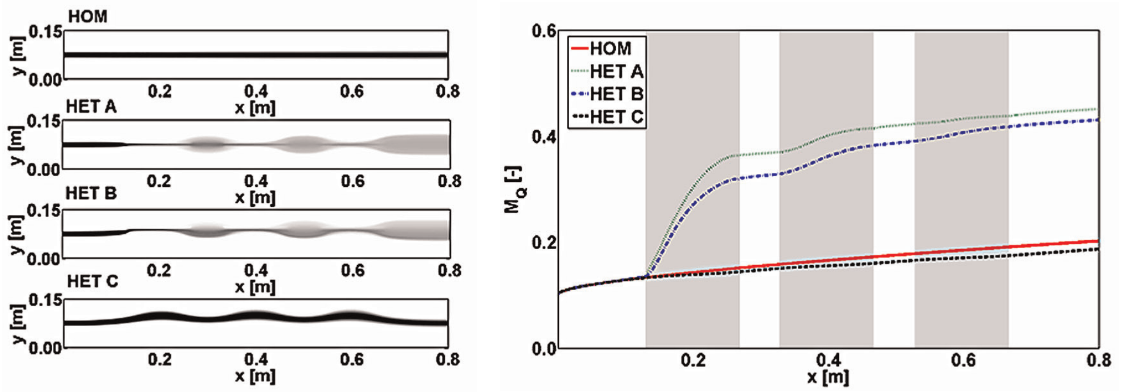

Figure 4. (left) Conservative plumes in the homogeneous bench-scale model (HOM) and in three heterogeneous cases (HET A, HET B, and HET C). (right) Computed reactor ratios (the gray regions indicate the location of the high permeability inclusions).

mass flux of the injected conservative tracer solution is diluted in the first inclusion. In the second heterogeneous case (Figure 4, HET B), the lenses are shifted toward the upper part of the system, and just the upper fringe of the plume is focused. The reduced focusing of the mass flux leads to a smoother increase in the flux-related reactor ratio. The effectiveness of the focusing decreases after each inclusion: the plume leaving the high-conductivity zone spreads over a wider region which is focused in a less efficient way by the successive inclusion (i.e., the mass flux involved in the flow focusing process decreases with the number of inclusions). In the last case (Figure 4, HET C), the plume is just meandering, but no effective focusing happens because of the presence of the heterogeneities since the mass flux of the tracer solution does not pass through the inclusions. In this case the mixing in the heterogeneous case is even slightly less effective than in the homogeneous one because the heterogeneities exclusively cause expansion of the plume. However, the flux-related reactor ratio is always a monotonically increasing function, while, for example, the second central spatial moment would decrease in the high conductivity inclusions, as shown by *Rolle et al.* [2009].

[34] In the field-scale setup, the plume can be focused by a higher number of high-conductivity lenses than in the bench-scale scenario. The average outcomes over 1000 realizations of binary heterogeneous flow fields, generated as previously described, are shown in Figure 5 as a solid line, and the shaded area indicates the range of ±1 standard deviation. While single realizations show a step-like increase in the reactor ratio (similar to the bench-scale simulations), the reactor ratio averaged over the entire ensemble of realizations behaves like the reactor ratio for a homogeneous system and can be fitted by equation (3). From the fitted inverse Péclet number we can evaluate the value of the effective transverse dispersion coefficient $D_{t,\mathrm{eff}} = 3.7 \times 10^{-8}$ m^2 s^{-1}. This coefficient represents the geometric mean of the effective mixing of the system because of local transverse dispersion enhanced by flow focusing. For a hydraulic conductivity contrast of 10, the mean value of the local dispersion coefficient, averaged over the entire domain, ($D_t = 6.3 \times 10^{-9}$ m^2 s^{-1}) is 6 times smaller than the effective one. We can thus conclude that over the ensemble average, the flow focusing effect increased the mixing capacity of the system by almost an order of magnitude. This result is in good agreement with the outcomes of reactive transport modeling studies at contaminated sites equipped with high-resolution monitoring wells [e.g., *Prommer et al.,* 2006, 2009]. For instance, in the coal tar–contaminated aquifer studied by *Prommer et al.* [2009], the best fit of the measured biogeochemical and isotopic gradients was obtained using a $D_t = 8.85 \times 10^{-8}$ m s^{-1} in the reactive transport simulations carried out in a two-dimensional homogeneous domain.

4.2. Results of Reactive Transport Simulations

[35] For a reactive system, we need to verify the validity of the definition of the equivalent homogeneous system given in section 3.2. Starting with the bench-scale simulations, we consider some of the scenarios presented in Figure 4 (i.e., the HOM, HET B, and HET C cases) with an inlet concentration of compound *A*, emitted from the source, equal to 1/6 of the ambient concentration of compound B in the ambient groundwater. Figure 6 shows the contour boundaries of the three reactive plumes and the dilution indices of the conservative tracer in the same system. In case HET B, the mass flux of compound *A* is focused in the inclusions, the mixing is enhanced in an efficient way, and the resulting plume is much shorter (0.15 m) than in the homogeneous setup. In case HET C, which presents the same high-permeability inclusions as HET B except shifted toward the upper boundary, the plume is bent because of the heterogeneous flow field and because just a negligible part of the fringe is focused, whereas the bulk plume exhibits only expansion because of the heterogeneities. As a result, the plume is even longer (0.78 m) than the homogeneous one (0.59 m). We conclude that knowing the overall degree of heterogeneity is not sufficient to quantify effects on mixing of an individual plume; one must know how the mass flux of the plume is affected by the flow field: if the plume is expanded rather than focused, then a heterogeneous system may even reduce the dilution of the plume.

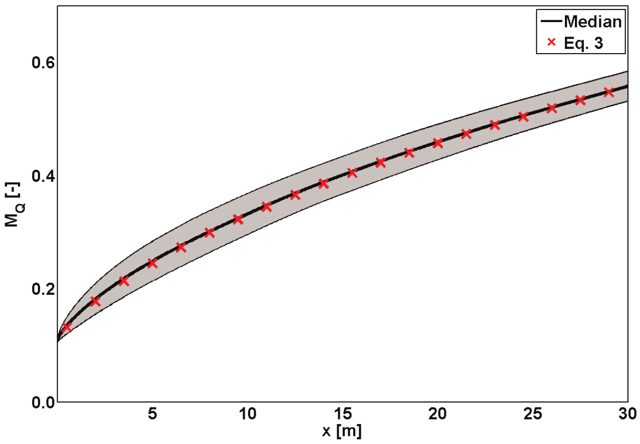

Figure 5. Average reactor ratio over 1000 realizations of the field-scale model. Shaded region represents ±1 standard deviation.

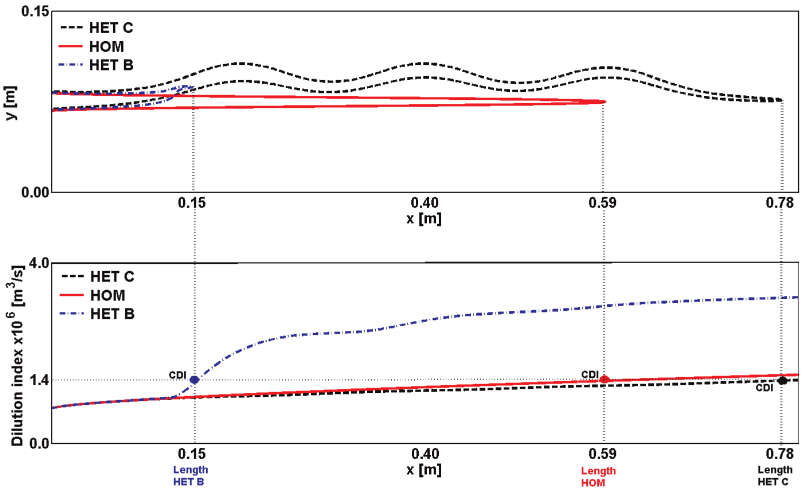

Figure 6. (top) Contours of three reactive plumes and (bottom) their flux-related and critical dilution index.

[36] It can be noticed that for a given mass flux of compound A, no difference can be detected between the values of the flux-related dilution index (i.e., the amount of mixing) at the length L of the reactive plume. This shows that even in extreme cases (complete focusing of the plume and bending with negligible focusing of a single fringe of the plume), the critical dilution index has the same value. We have to point out that in order to correctly quantify the value of the critical dilution index, the numerical dispersion of the code must be negligible. In fact, the value of E_Q is the exponential of the entropy of the system, and hence, even a small numerical error may strongly affect this quantity if computed through numerical simulations.

[37] In order to test the hypothesis that the value of the critical dilution index does not depend significantly on the heterogeneity of the system, we generated 1000 random conductivity fields with a conductivity contrast of 10, as previously described. These realizations were performed at the larger field scale. The statistical analysis of the results (i.e., a chi-square goodness of fit test) shows that the values of the reactive plume length and the related effective transverse dispersion (equation (11)) are lognormal distributed (Figure 7). The smaller the value of X_{crit}, the longer the plume is, and hence, the plume can sample a higher number of heterogeneities of the flow field before the end of the reactive plume is reached. This reduces the variability of the effective transverse dispersion coefficient and of the plume length within the ensemble of realizations (in fact, $\sigma_{\ln(L)}$ and $\sigma_{\ln(D_{t,\mathrm{eff}})}$ must be equal because of equation (11)). On the contrary, the shorter the plume (i.e., the larger X_{crit} is), the larger the variability of the effective transverse dispersion coefficient among the realizations is. For the same reason, for small values of X_{crit} (i.e., long plumes) we obtain a slightly higher geometric mean of the effective transverse dispersion coefficients derived in the heterogeneous cases (equation (11)), and hence, we have a slight dependency of $D_{t,\mathrm{eff}}$ on X_{crit}.

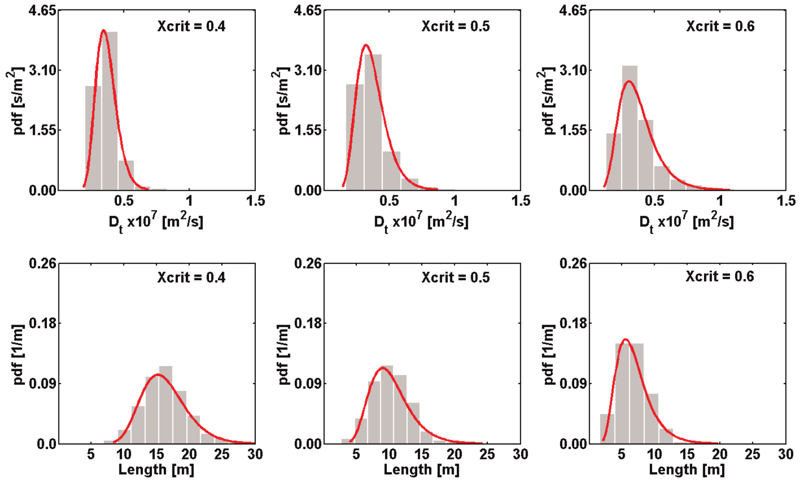

Figure 7. Probability density functions and histograms (top) of the effective transverse dispersion coefficient and (bottom) of the reactive plume length computed over the ensemble of 1000 realizations of field-scale heterogeneous domains for different values of X_{crit}.

Table 3. Relationship Between X_{crit}, Plume Length, and Effective Transverse Dispersion Coefficient, with the Standard Deviations of the Logarithm of Their Distribution $\sigma_{\ln(D_{t,\mathrm{eff}})}$ and $\sigma_{\ln(L)}$, Respectively

X_{crit}	Geometric Mean of the Plume Length L (m)	Geometric Mean of the Effective Transverse Dispersion Coefficient $D_{t,\mathrm{eff}}$ ($\times 10^7$ m^{2}s^{-1})	$\sigma_{\ln(D_{t,\mathrm{eff}})}$ and $\sigma_{\ln(L)}$
Conservative	-	0.38	-
0.4	16.1	0.36	0.2
0.5	10.1	0.35	0.3
0.6	6.5	0.34	0.4

[38] Table 3 shows this slight dependence of $D_{t,\mathrm{eff}}$ on X_{crit} and thus on the reaction stoichiometry and the concentrations of the reaction partners in the inflow. It is worth noting that the determination of the effective dispersion coefficient using the flux-related dilution index (i.e., for conservative transport) and analyzing the reactive cases leads to very close results. Other methods to determine an upscaled dispersion coefficient usually are not able to predict a correct effective dispersion coefficient for reactive transport [*Cirpka*, 2002]. In the numerical simulations, the value of the logarithm of the flux-related dilution index (i.e., the entropy of the conservative mass flux) at the end of the plume for the heterogeneous case and the equivalent homogeneous case remains almost identical, showing an average difference of ±0.4%. That is, in most cases, the distributions of p_Q for the homogeneous and the heterogeneous cases have not only the same maximum (per construction) but also the same entropy, so that the concept of the critical dilution index appears valid. Although it is mathematically possible to construct distributions with significantly different entropy but identical maximum, our numerical experiment indicates that physical constraints of solute transport (e.g., the diffusive nature of the governing equation, typical values of the parameters involved such as the velocity and the local dispersion coefficient, natural heterogeneity patterns, etc.) strongly limit and generally avoid the occurrence of such distributions.

[39] Taking the geometric mean over the ensemble of realizations, the relation between X_{crit}, L, and the effective transverse dispersion coefficient $D_{t,\mathrm{eff}}$ is the same as equation (11) (Figure 7):

$$LD_{t,\mathrm{eff}} = \frac{vw^2}{16\mathrm{inverf}(X_{\mathrm{crit}})^2}, \qquad (13)$$

where w is the effective width of the line source in the equivalent homogeneous case, $D_{t,\mathrm{eff}}$ is the geometric mean of the effective transverse dispersion coefficient of the equivalent homogeneous systems, and L is the geometric mean of the length of plumes in the heterogeneous simulations. The average seepage velocity v is constant for all realization since we keep the discharge of the system constant. The product between the plume length and the effective dispersion coefficient is per construction univocally determined for a given X_{crit} (Figure 8).

[40] The results of the simulations confirm that the critical dilution index and the critical mixing ratio are related as predicted by equation (10) (Figure 8) for a given mass flux at the source. There is a small deviation from the expected values for high X_{crit} (i.e., short plumes) that can be explained by the fact that equation (10) is a first-order approximation for small values of X_{crit}. We have to consider, furthermore, that the validity of the analytical solution of *Domenico and Palciauskas* [1982] is not given in the proximity of the source [*Srinivasan et al.*, 2007].

[41] Table 4 lists results for three different conductivity contrasts. These results indicate that the critical dilution index remains constant if the mass flux of the injected compound is the same; it only depends on the critical mixing ratio of the system (Table 4), as correctly predicted by equation (10). Hence, the definition given for the equivalent homogeneous system is reasonable since it allows obtaining a very good approximation for the dilution required for complete reaction of a plume even in heterogeneous systems with different permeability contrasts. The distributions of the plume length and of the effective transverse dispersion coefficient are affected by a higher uncertainty if the conductivity contrast is higher. For instance, given a conductivity contrast of 10, $\sigma_{\ln(L)}$ varies between 0.2 and 0.3 for $X_{\mathrm{crit}} = 0.4$ and $X_{\mathrm{crit}} = 0.5$, respectively; for a conductivity contrast of 30 and the same values of X_{crit},

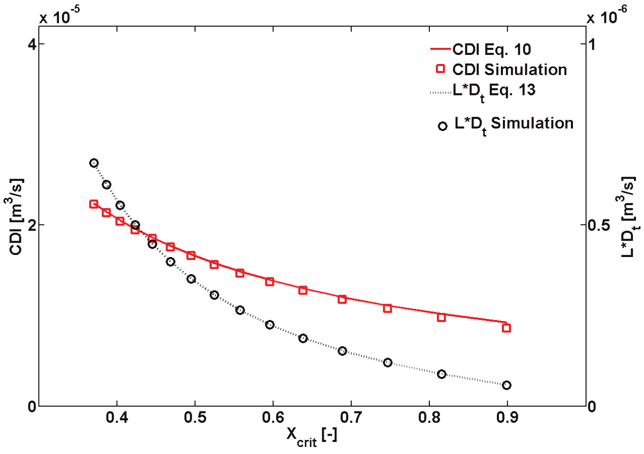

Figure 8. Relations between the critical dilution index (CDI) and X_{crit} and between the product LD_t and X_{crit}. The geometric mean over 1000 realizations is plotted for the numerical simulation results.

Table 4. Influence of the Hydraulic Conductivity Contrast ($K_{\text{high}}/K_{\text{low}}$) on $D_{t,\text{eff}}$, the Plume Length L, and the Critical Dilution Index (CDI) for Different X_{crit} (Geometric Mean Values)

	$K_{\text{high}}/K_{\text{low}} = 10$			$K_{\text{high}}/K_{\text{low}} = 20$			$K_{\text{high}}/K_{\text{low}} = 30$		
X_{crit}	0.40	0.45	0.50	0.40	0.45	0.50	0.40	0.45	0.50
$D_{t,\text{eff}}$ ($\times 10^7$ m^2 s^{-1})	0.36	0.35	0.35	0.68	0.67	0.66	0.96	0.91	0.87
Length (m)	16.1	12.5	10.19	8.4	6.5	5.2	5.9	4.8	3.9
CDI ($\times 10^4$ m^3 s^{-1})	0.21	0.18	0.17	0.21	0.18	0.17	0.21	0.18	0.17

the variance $\sigma_{\ln(L)}$ of the log plume length varies between 0.3 and 0.4. Heterogeneous fields with higher conductivity contrast (and thus more effective flow focusing) result generally in shorter plumes and higher effective dispersion coefficients. We can note that the effective transverse dispersion coefficient in this setup increases almost linearly with the permeability contrast.

5. Conclusion

[42] In this study, we illustrated the concept of flux-related dilution index, which is an appropriate measure to quantify mixing in both homogeneous and heterogeneous systems into which a conservative solute is continuously injected. For reactive systems, we introduced the critical dilution index, which is the degree of mixing required for the complete degradation of a reactive plume in the case of instantaneous complete bimolecular reactions. In homogenous systems, the critical dilution index can be computed analytically. In order to transfer the concept of the critical dilution index to heterogeneous porous media, we have defined an equivalent homogeneous system in which the effective transverse dispersion coefficient is the one that matches the length of the plume. The results of the numerical simulations show that in this way it is possible to extend the use of the critical dilution index to heterogeneous systems. The newly defined effective transverse dispersion coefficient of the equivalent homogenous porous medium depends on the permeability contrast of the system and, via the critical mixing ratio, on the stoichiometry of the reaction, as well as the inflow and ambient concentrations. The local dispersion coefficient can be substantially smaller than the effective dispersion coefficient derived as a fitting parameter to simulate the behavior of reactive plumes in heterogeneous formations. In our opinion, the apparent scale dependency of the transverse dispersion coefficient, which appears in the interpretation of field-scale plumes, is caused by the difficulty in capturing correctly the flow field when flow focusing effects caused by advective heterogeneities are the dominant mixing enhancement process. Furthermore, we showed that information about the mass flux of a solute is of utmost importance in order to predict the fate of contaminant plumes. The performed theoretical and numerical analysis helps to answer the questions we posed in section 3.2.

[43] 1. The mixing of a conservative and of a reactive tracer can be quantitatively related to each other by the concept of critical dilution index in moderately heterogeneous aquifers and for instantaneous complete bimolecular reactions.

[44] 2. The flux-related dilution index of the system can be calculated from a conservative tracer. Under the assumption of instantaneous, mixing-controlled reactions, we can predict where a reactive plume generated by a continuous source will end if we know the critical dilution index of the system. In heterogeneous systems, information about the mass flux is required in order to correctly estimate the dilution of steady state plumes, whereas the knowledge of the spatial concentration distribution alone is not sufficient.

[45] 3. The amount of mixing required to completely degrade a reactive plume is well approximated by the value of the critical dilution index, a quantity that is exclusively controlled by the critical mixing ratio of the system and by the mass flux of the injected reactive species. The critical dilution index is defined over a cross section of the domain. Hence, it is not required to map the whole heterogeneity of an aquifer system if we can quantify the mass flux of a plume over the cross section where the critical value for dilution is reached.

[46] As already pointed out by *Kitanidis* [1994], the possibility to define a dilution index has a significant impact on many engineering applications, such as the design and optimization of in situ remediation applications. With this work, we have added important information in order to answer the question whether it is possible to predetermine how much mixing is necessary to let a contaminant plume degrade. The determination of the critical dilution index and of the flux-related dilution index may be challenging in practical applications because of the difficulties in measuring mass fluxes, determining the geometry of the source, and estimating the concentrations of the reaction partners. Nonetheless, any reactive transport model already contains this information as an input (e.g., initial concentration of the reactive species and source geometry), or it can be easily computed (such as the mass fluxes of the different chemical species). So the direct computation of the critical and the flux-related dilution indices, which can be performed on the basis of only conservative transport, will be useful when assessing plume development and/or potential remediation interventions on the basis of a modeling study.

[47] The study of the behavior of the critical dilution index in cases of different reaction kinetics, of noncomplete equilibrium reactions, of reaction partners with different aqueous diffusion coefficients, and when the effects of transient flow on the effective dispersion tensor are relevant [e.g., *Cirpka and Attinger*, 2003; *Dentz and Carrera*, 2005] requires further investigation.

Appendix A: Transport of the Entropy Density

[48] In this appendix, we derive the transport equation for the entropy density $p_Q \ln(p_Q)$ of a conservative component. In the case of steady state transport, the probability density function p_Q, as defined in Table 1, must satisfy the following conservation equation:

$$\nabla \cdot \left(\mathbf{q} p_Q - n\mathbf{D}\nabla p_Q\right) = 0. \tag{A1}$$

[49] Multiplying equation (A1) by ln p_Q and applying the chain rule of differentiation, we obtain the following equation for the advective and dispersive fluxes:

$$\ln p_Q \nabla \cdot \left(\mathbf{q} p_Q\right) = \nabla \cdot \left(\mathbf{q} p_Q \ln p_Q\right) - \nabla \cdot \left(\mathbf{q} p_Q\right) \tag{A2}$$

$$\begin{aligned}\ln p_Q \nabla \cdot \left(n\mathbf{D}\nabla p_Q\right) = \nabla \cdot \left[n\mathbf{D}\nabla\left(p_Q \ln p_Q\right)\right] - \nabla \cdot \left(n\mathbf{D}\nabla p_Q\right) \\ - \frac{1}{p_Q}\left(\nabla p_Q\right)^T n\mathbf{D}\left(\nabla p_Q\right).\end{aligned} \tag{A3}$$

[50] Hence, combining equations (A1), (A2), and (A3), we obtain an advection-dispersion equation for the entropy with a source term

$$\nabla \cdot \left(\mathbf{q} p_Q \ln p_Q - n\mathbf{D}\nabla p_Q \ln p_Q\right) = -p_Q \nabla \ln p_Q{}^T n\mathbf{D}\nabla \ln p_Q. \tag{A4}$$

[51] Integrating equation (A4) over the unbounded cross section perpendicular to the main direction of the flow, we obtain (remembering that we defined $q = q_{\mathrm{x}}$)

$$\begin{aligned}&\frac{\mathrm{d}}{\mathrm{d}x}\int_{\infty}\left(q p_Q \ln p_Q - \mathbf{e}_1^T n\mathbf{D}\nabla p_Q \ln p_Q\right)\mathrm{d}y\mathrm{d}z \\ &= -\int_{\infty} p_Q \nabla \ln p_Q{}^T n\mathbf{D}\nabla \ln p_Q \mathrm{d}y\mathrm{d}z \\ &= -\int_{\infty} \frac{1}{p_Q}\nabla p_Q{}^T n\mathbf{D}\nabla p_Q \mathrm{d}y\mathrm{d}z.\end{aligned} \tag{A5}$$

[52] In the advection-dominated case we can neglect the second term of the left-hand side integrand, so that the rate of increase of the flux-related dilution index with respect to the main direction of the flow is

$$\begin{aligned}\frac{\mathrm{d}F_{p_Q \ln p_Q}}{\mathrm{d}x} &\approx \frac{\mathrm{d}}{\mathrm{d}x}\int_{\infty}\left(q p_Q \ln p_Q\right)\mathrm{d}y\mathrm{d}z = \frac{\mathrm{d}\ln E_Q}{\mathrm{d}x} \\ &= -\int_{\infty} p_Q \nabla \ln p_Q{}^T n\mathbf{D}\nabla \ln p_Q \mathrm{d}y\mathrm{d}z,\end{aligned} \tag{A6}$$

where $F_{p_Q \ln p_Q}$ is the total entropy flux integrated over a cross-sectional area.

Appendix B: Relationship Between Flux-Related and Cross-Sectional Dilution Indices in Homogeneous Cases

[53] In this appendix, we show how to relate the flux-related dilution index to the cross-sectional dilution index in a homogeneous porous medium. The flux-related dilution index is defined as

$$E_Q(x) = \exp\left\{-\int_A p_Q(\mathbf{x})\ln\left[p_Q(\mathbf{x})\right]q_x(\mathbf{x})\mathrm{d}y\mathrm{d}z\right\}. \tag{B1}$$

[54] In a homogeneous domain, the volumetric flux is uniformly distributed along the cross section, so we can write

$$E_Q(x) = \exp\left\{-\int_A \frac{p(\mathbf{x})}{q_x(\mathbf{x})}\ln\left[\frac{p(\mathbf{x})}{q_x(\mathbf{x})}\right]q_x(\mathbf{x})\mathrm{d}y\mathrm{d}z\right\}. \tag{B2}$$

[55] And hence

$$\begin{aligned}E_Q(x) &= \exp\left(-\int_A \{p(\mathbf{x})\ln[p(\mathbf{x})] - p(\mathbf{x})\ln[q_x(\mathbf{x})]\}\mathrm{d}y\mathrm{d}z\right) \\ &= E_{cs}(x)q_x(\mathbf{x}).\end{aligned} \tag{B3}$$

[56] If we now change to a coordinate system moving with velocity v, so that $x = vt$, we obtain

$$E_Q(x) = E_{\mathrm{cs}}(vt)q_x(vt). \tag{B4}$$

Appendix C: Flux-Related Dilution Index for a Line Source in Homogeneous Two-Dimensional Domains and Analytical Expressions for Other Remarkable Cases

[57] In the following, we derive the semianalytical equation to express the flux-related dilution index in case of a line source, and we present some analytical expressions for other remarkable cases. We assume that the value of the flux-related dilution index can be expressed by a nested radical of the form

$$\begin{aligned}&E_Q(L) = wZq_x \\ &\times\left(1+\sqrt{ax+(n+a)^2+x\sqrt{a(x+n)+(n+a)^2+(x+n)\sqrt{\ldots}}}\right),\end{aligned} \tag{C1}$$

where w is the source width in the y direction and Z is the thickness of the system in the z direction. The fitted coefficients a, x, and n have the following values:

$$\begin{aligned}a &= 0, \\ n &= \sqrt{4\pi\exp(1)\varepsilon_y(L)}, \\ x &= -\sqrt{\frac{4\pi\varepsilon_y}{4\pi\varepsilon_y+1}},\end{aligned} \tag{C2}$$

where ε_y is defined as in equation (4), i.e., $\varepsilon_y = nxD_t/(q_x w^2)$.

[58] We note that the nested radical is the general formulation of the Ramanujan identity [*Ramanujan*, 1911], which can be simplified through

$$E_Q(\varepsilon_y) = wZq_x\left(1-\sqrt{\frac{\varepsilon_y}{\varepsilon_y+\exp(1)}}+\sqrt{4\pi\exp(1)\varepsilon_y}\right). \tag{C3}$$

[59] Equation (C3) converges for the limit $w \to 0$ to the expected analytical solution given by equation (C8) for the limit $x \to 0$ to the dilution index at the source (i.e., the value of the exponential of the entropy of a uniform distribution), and it fits in an excellent way the results of the numerical simulations (Figure 1).

[60] It is worth noting that the inverse Péclet number can be expressed as

$$\varepsilon_y(L) = \frac{1}{16\mathrm{inverf}(X_{\mathrm{crit}})^2} \tag{C4}$$

if we are far enough from the source zone (i.e., the hypothesis underlying equation (8) is satisfied [*Srinivasan et al.*, 2007]). This requirement is satisfied for small values of X_{crit}. If we truncate the Taylor expansion of the $\mathrm{inverf}(X_{\mathrm{crit}})$ at its first order, we obtain

$$\mathrm{inverf}(X_{\mathrm{crit}}) = \frac{1}{2}\sqrt{\pi}X_{\mathrm{crit}} + O\left(X_{\mathrm{crit}}{}^3\right). \tag{C5}$$

[61] It is now straightforward to compute the first-order approximation for the critical dilution index:

$$\mathrm{CDI} \equiv E_Q(L) = \frac{E_Q(0)}{X_{\mathrm{crit}}}\exp(1/2). \tag{C6}$$

[62] This value is exactly the value of the critical dilution index we expect for a Gaussian plume. Hence, equation (A1) satisfies the convergence for long plumes to a Gaussian shape.

[63] The values of $E_Q(x)$ for the case of uniform flow with a continuous point injection can be computed from the analytical expressions given by *Kitanidis* [1994] (equations (C3) and (C4)). In a 3-D unbounded domain with uniform flow in direction x, we obtain, for a point-like injection,

$$E_Q(x) = 4\pi\exp(1)xnD_t, \tag{C7}$$

where n (dimensionless) is the porosity of the system and D_t $[L^2\,T^{-1}]$ is the local transverse dispersion coefficient.

[64] In a two-dimensional domain with thickness Z $[L]$, we obtain, for an injection over the thickness,

$$E_Q(x) = \exp(1/2)Z\sqrt{4\pi xnD_tq_x}. \tag{C8}$$

[65] That is, in the unbounded 3-D uniform case, the flux-related dilution index increases linearly with distance, whereas in the case of 2-D flow we obtain an expression scaling with the square root of the travel distance.

Appendix D: Uniqueness of the Critical Dilution Index in Homogeneous Media

[66] In this appendix, we compute the critical dilution index in the homogeneous case and prove its uniqueness independent from the transverse dispersion coefficient. We consider the same reactive system (i.e., same stoichiometric coefficients, same flow conditions, same source geometry, etc.) for two different transverse dispersion coefficients (e.g., two packed beds with two distinct grain sizes), and we work under the hypothesis that the validity conditions of equations (8) and (9) apply.

[67] The plume length L is different since it depends on the transverse dispersion coefficients:

$$\begin{aligned} L_1 &= \frac{vw^2}{16D_{t1}\mathrm{inverf}(X_{\mathrm{crit}})^2} \\ L_2 &= \frac{vw^2}{16D_{t2}\mathrm{inverf}(X_{\mathrm{crit}})^2}. \end{aligned} \tag{D1}$$

[68] We consider the analytical solution [*Domenico and Palciauskas*, 1982] for the two conservative cases, with initial concentration C_0 $[M\,L^{-3}]$:

$$\frac{C_i(x,y)}{C_0} = \frac{1}{2}\left[\mathrm{erf}\left(\frac{y+\frac{w}{2}}{2\sqrt{D_{ti}\frac{x}{v}}}\right) - \mathrm{erf}\left(\frac{y-\frac{w}{2}}{2\sqrt{D_{ti}\frac{x}{v}}}\right)\right], \quad i = 1,2. \tag{D2}$$

[69] If we compute the concentration of the conservative tracer at $x = L_1$ and $x = L_2$, we obtain

$$\frac{C_1(L_1,y)}{C_0} = \frac{1}{2}\left[\mathrm{erf}\left(\frac{y+\frac{w}{2}}{2\sqrt{\frac{w^2}{16\mathrm{inverf}(X_{\mathrm{crit}})}}}\right) - \mathrm{erf}\left(\frac{y-\frac{w}{2}}{2\sqrt{\frac{w^2}{16\mathrm{inverf}(X_{\mathrm{crit}})}}}\right)\right]. \tag{D3}$$

[70] The same procedure can be applied to compute the concentration for the second case:

$$\frac{C_2(L_2,y)}{C_0} = \frac{1}{2}\left[\mathrm{erf}\left(\frac{y+\frac{w}{2}}{2\sqrt{\frac{w^2}{16\mathrm{inverf}(X_{\mathrm{crit}})}}}\right) - \mathrm{erf}\left(\frac{y-\frac{w}{2}}{2\sqrt{\frac{w^2}{16\mathrm{inverf}(X_{\mathrm{crit}})}}}\right)\right]. \tag{D4}$$

[71] So we have demonstrated that

$$C_1(L_1,y) = C_2(L_2,y). \tag{D5}$$

[72] We compute the probability density function for the flux-related dilution index,

$$p_Q(x,y) = \frac{C(x,y)}{\int q_xC(x,y)\mathrm{d}x\mathrm{d}y}, \tag{D6}$$

and we note that

$$p_{Q_1}(L_1,y) = \frac{C_1(L_1,y)}{\int q_xC_1(L_1,y)\mathrm{d}y} = \frac{C_2(L_2,y)}{\int q_xC_2(L_2,y)\mathrm{d}y} = p_{Q_2}(L_2,y). \tag{D7}$$

[73] Hence, it is straightforward to demonstrate that the critical dilution index must assume the same value in homogenous porous media:

$$\mathrm{CDI}(L_1) = E_Q(L_1) = E_Q(L_2) = \mathrm{CDI}(L_2). \tag{D8}$$

[74] **Acknowledgments.** We thank Al Valocchi and two anonymous reviewers for their constructive and helpful comments. Support from the Deutsche Forschungsgemeinschaft (DFG) Research Group FOR 525

"Analysis and modeling of diffusion/dispersion-limited reactions in porous media" (grants GR971/18-1 and GR971/18-3) is gratefully acknowledged.

References

Anneser, B., F. Einsiedl, R. U. Meckenstock, L. Richters, F. Wisotzky, and C. Griebler (2008), High-resolution monitoring of biogeochemical gradients in a tar oil-contaminated aquifer, *Appl. Geochem.*, *23*, 1715–1730.

Bauer, R. D., M. Rolle, S. Bauer, C. Eberhardt, P. Grathwohl, O. Kolditz, R. U. Meckenstock, and C. Griebler (2009), Enhanced biodegradation by hydraulic heterogeneities in petroleum hydrocarbon plumes, *J. Contam. Hydrol.*, *105*, 56–68.

Bear, J. (1972), *Dynamics of Fluids in Porous Media*, Dover, New York.

Bear, J., and Y. Sun (1998), Optimization of pump-treat-inject (PTI) design for the remediation of a contaminated aquifer: Multi-stage design with chance constraints, *J. Contam. Hydrol.*, *29*, 225–244.

Beckie, R. D. (1998), Analysis of scale effects in large-scale solute transport models, in *Scale Dependence and Scale Invariance in Hydrology*, edited by G. Sposito, pp. 314–334. Cambridge Univ. Press, New York.

Bloem, E., F. A. N. Hogervorst, and G. H. de Rooij (2009), A field experiment with variable-suction multi-compartment samplers to measure the spatio-temporal distribution of solute leaching in an agricultural soil, *J. Contam. Hydrol.*, *105*, 131–145.

Cao, J., and P. K. Kitanidis (1998), Pore-scale dilution of conservative solutes: An example, *Water Resour. Res.*, *34*, 1941–1949.

Chilakapati, A., and S. Yabusaki (1999), Nonlinear reactions and nonuniform flows, *Water Resour. Res.*, *35*, 2427–2438.

Chiogna, G., M. Rolle, O. A. Cirpka,and P. Grathwohl (2010a), Modeling mixing-controlled reactive transport: Importance of compound dependent hydrodynamic and (hydro)mechanical transverse dispersion, paper presented at XVIII International Conference on Computational Methods in Water Resources, CIMNE, Barcelona, Spain.

Chiogna, G., C. Eberhardt, P. Grathwohl, O. A. Cirpka, and M. Rolle (2010b), Evidence of compound dependent hydrodynamic and mechanical transverse dispersion by multitracer laboratory experiments, *Environ. Sci. Technol.*, *44*, 688–693, doi:10.1021/es9023964.

Cirpka, O. A. (2002), Choice of dispersion coefficients in reactive transport calculations on smoothed fields, *J. Contam. Hydrol.*, *58*, 261–282.

Cirpka, O. A., and S. Attinger (2003), Effective dispersion in heterogeneous media under random transient flow conditions, *Water Resour. Res.*, *39*(9), 1257, doi:10.1029/2002WR001931.

Cirpka, O. A., and A. J. Valocchi (2007), Two-dimensional concentration distribution for mixing-controlled bioreactive transport in steady state, *Adv. Water Resour.*, *30*, 1668–1679.

Cirpka, O. A., E. O. Frind, and R. Helmig (1999a), Numerical simulation of biodegradation controlled by transverse mixing, *J. Contam. Hydrol.*, *40*, 159–182.

Cirpka, O. A., E. O. Frind, and R. Helmig (1999b), Streamline-oriented grid-generation for transport modelling in two-dimensional domains including wells, *Adv. Water Resour.*, *22*, 697–710.

Cirpka, O. A., R. Helmig, and E. O. Frind (1999c), Numerical methods for reactive transport on rectangular and streamline-oriented grids, *Adv. Water Resour.*, *22*, 711–728.

Cirpka, O. A., A. Olsson, Q. Ju, A. Rahman, and P. Grathwohl (2006), Determination of transverse dispersion coefficients from reactive plumes lengths, *Ground Water*, *44*, 212–221.

Dagan, G. (1984), Solute transport in heterogeneous porous formations, *J. Fluid Mech.*, *145*, 151–177.

Dagan, G. (1990), Transport in heterogeneous porous formations: Spatial moments, ergodicity, and effective dispersion, *Water Resour. Res.*, *26*, 1281–1290.

Dagan, G. (1991), Dispersion of a passive solute in nonergodic transport by steady velocity-fields in heterogeneous formations, *J. Fluid Mech.*, *233*, 197–210.

Davis, T. A., and I. S. Duff (1997), An unsymmetric-pattern unifrontal method for sparse LU factorization, *SIAM J. Matrix Anal. Appl.*, *18*, 140–158.

de Barros, F. P. J., and W. Nowak (2010), On the link between contaminant source release conditions and plume prediction uncertainty, *J. Contam. Hydrol.*, *116*(1–4), 24–34.

Dentz, M., and J. Carrera (2003), Effective dispersion in temporally fluctuating flow through a heterogeneous medium, *Phys. Rev. E*, *68*, 036310.

Dentz, M., and J. Carrera (2005), Effective solute transport in temporally fluctuating flow through heterogeneous media, *Water Resour. Res.*, *41*, W08414. doi:10.1029/2004WR003571.

Dentz, M., H. Kinzelbach, S. Attinger, and W. Kinzelbach (2000a), Temporal behavior of a solute cloud in a heterogeneous porous medium: 1. Point-like injection, *Water Resour. Res.*, *36*, 3591–3604.

Dentz, M., H. Kinzelbach, S. Attinger, and W. Kinzelbach (2000b) Temporal behavior of a solute cloud in a heterogeneous porous medium: 2. Spatially extended injection, *Water Resour. Res.*, *36*, 3605–3614.

de Rooij, G. H., O. A. Cirpka, F. Stagnitti, S. H. Vuurens, and J. Boll (2006), Quantifying minimum monolith size and solute dilution from multi-compartment percolation sampler data, *Vadose Zone J.*, *5*, 1086–1092.

De Simoni, M., J. Carrera, X. Sanchez-Vila, and A. Guadagnini (2005), A procedure for the solution of multi-component reactive transport problems, *Water Resour. Res.*, *41*, W11410. doi:10.1029/2005WR004056.

De Simoni, M., X. Sanchez-Vila, J. Carrera, and M.W. Saaltink (2007), A mixing ratios-based formulation for multicomponent reactive transport, *Water Resour. Res.*, *43*, W07419. doi:10.1029/2006WR005256.

Domenico, P. A., and V. V. Palciauskas (1982), Alternative boundaries in solid waste management, *Ground Water*, *20*, 303–311.

Gelhar, L. W., and C. L. Axness (1983), Three-dimensional stochastic analysis of macrodispersion in aquifers, *Water Resour. Res.*, *19*, 161–180.

Kapoor, V., and P. K. Kitanidis (1996), Concentration fluctuations and dilution in two-dimensionally periodic heterogeneous porous media, *Transp. Porous Media*, *22*, 91–119.

Kapoor, V., and P. K. Kitanidis (1998), Concentration fluctuations and dilution in aquifers, *Water Resour. Res.*, *34*, 1181–1193.

Kitanidis, P. K. (1988), Prediction by the method of moments of transport in heterogeneous formations, *J. Hydrol.*, 102, 453–473.

Kitanidis, P. K. (1994), The concept of dilution index, *Water Resour. Res.*, *30*, 2011–2026.

Klenk, I. D., and P. Grathwohl (2002), Transverse vertical dispersion in groundwater and the capillary fringe, *J. Contam. Hydrol.*, *58*, 111–128.

Kreft, A., and A. Zuber (1978), On the physical meaning of the dispersion equation and its solutions for different initial and boundary conditions, *Chem. Eng. Sci.*, *33*, 1471–1480.

Lerner, D. N., S. F. Thornton, M. J. Spence, S. A. Banwart, S. H. Bottrell, J. J. Higgo, H. E. H. Mallinson, R. W. Pickup, and G. M. Williams (2000), Ineffective natural attenuation of degradable organic compounds in a phenol-contaminated aquifer, *Ground Water*, *38*, 922–928.

Liedl, R., A. J. Valocchi, P. Dietrich, and P. Grathwohl (2005), Finiteness of steady state plumes, *Water Resour. Res.*, *41*, W12501. doi:10.1029/2005WR004000.

McLaughlin, D., and F. Ruan (2001), Macrodispersivity and large-scale hydrogeologic variability, *Transp. Porous Media*, *42*, 133–154.

Moroni, M., N. Kleinfelter, and J. H. Cushman (2007), Analysis of dispersion in porous media via matched-index particle tracking velocimetry experiments, *Adv. Water Res.*, *30*, 1–15.

Neuman, S. P., C. L. Winter, and C. M. Newman (1987), Stochastic theory of field-scale Fickian dispersion in anisotropic porous media, *Water Resour. Res.*, *23*, 453–466.

Pannone, M., and P. K. Kitanidis (1999), Large-time behavior of concentration variance and dilution in heterogeneous formations, *Water Resour. Res.*, *35*, 623–634.

Prommer, H., N. Tuxen, and P. Bjerg (2006), Fringe-controlled natural attenuation of phenoxy acids in a landfill plume: Integration of field-scale processes by reactive transport modelling, *Environ. Sci. Technol.*, *40*, 4732–4738.

Prommer, H., B. Anneser, M. Rolle, F. Einsiedl, and C. Griebler (2009), Biogeochemical and isotopic gradients in a BTEX/PAH contaminant plume: Model-based interpretation of a high-resolution field data set, *Environ. Sci. Technol.*, *43*, 8206–8212.

Rahman, A. M., S. Jose, W. Nowak, and O. A. Cirpka (2005), Experiments on vertical transverse mixing in a large-scale heterogeneous model aquifer. *J. Contam. Hydrol.*, *80*, 130–148, doi:10.1016/j.jconhyd.2005.06.010.

Rajaram, H., and L. W. Gelhar (1993a), Plume scale-dependent dispersion in heterogeneous aquifers: 1. Lagrangian analysis in a stratified aquifer, *Water Resour. Res.*, *29*, 3249–3260.

Rajaram, H., and L. W. Gelhar (1993b), Plume scale-dependent dispersion in heterogeneous aquifers: 2. Eulerian analysis and three-dimensional aquifers, *Water Resour. Res.*, *29*, 3261–3276.

Rajaram, H., and L. W. Gelhar (1995), Plume-scale dispersion in aquifers with a wide range of scales of heterogeneity, *Water Resour. Res.*, *31*, 2469–2482.

Ramanujan, S. (1911), Question No. 298. *J. Indian Math. Soc.*, *3*, 90.

Rolle, M., C. Eberhardt, G. Chiogna, O. A. Cirpka, and P. Grathwohl (2009), Enhancement of dilution and transverse reactive mixing in porous media: Experiments and model-based interpretation, *J. Contam. Hydrol.*, *110*, 130–142.

Rolle, M., G. Chiogna, R. Bauer, C. Griebler, and P. Grathwohl (2010), Isotopic fractionation by transverse dispersion: Flow-through microcosms and reactive transport modeling study, *Environ. Sci. Technol.*, *44*, 6167–6173.

Rossi, M., P. Lehmann, N. Ursino, O. Ippisch, and H. Flühler (2007), Solute mixing during imbibition and drainage in a macroscopically heterogeneous medium, *Water Resour. Res.*, *43*, W04428. doi:10.1029/2005WR004038.

Rossi, M., O. Ippisch, and H. Flühler (2008), Solute dilution under imbibition and drainage conditions in a heterogeneous structure: Modeling of a sand tank experiment, *Adv. Water Resour.*, *31*, 1242–1252.

Scheidegger, A. E. (1961), General theory of dispersion in porous media, *J. Geophys. Res.*, *66*, 3273–3278.

Srinivasan, V., T. P. Clement, and K. K. Lee (2007), Domenico solution—Is it valid?, *Ground Water*, *45*, 136–146.

Tartakovsky, A. M., G. D. Tartakovsky, and T. D. Scheibe (2009), Effects of incomplete mixing on multicomponent reactive transport, *Adv. Water Resour.*, *32*, 1674–1679.

Thierrin, J., and P. K. Kitanidis (1994), Solute dilution at the Borden and Cape Cod groundwater tracer tests, *Water Resour. Res.*, *30*, 2883–2890.

Ursino, N., T. Gimmi, and H. Flühler (2001), Dilution of nonreactive tracers in variably saturated sandy structures, *Adv. Water Resour.*, *24*, 877–885.

Valocchi, A. J., K. Nakshatrala, and M. Massabò (2009), Reactions along transverse mixing zones in heterogeneous aquifers: Using effective dispersion coefficients and multi-scale finite element methods, *Eos Trans. AGU*, *90*(52), Fall Meet. Suppl., Abstract H32C-04.

Werth, C. J., O. A Cirpka, and P. Grathwohl (2006), Enhanced mixing and reaction through flow focusing in heterogeneous porous media, *Water Resour. Res.*, *42*, W12414. doi:10.1029/2005WR004511.

Willingham, T. W., C. J. Werth, and A. J. Valocchi (2008), Evaluation of the effects of porous media structure on mixing-controlled reactions using pore-scale modeling and micromodel experiments, *Environ. Sci. Technol.*, *42*, 3185–3193.

Willingham, T., C. Zhang, C. J. Werth, A. J. Valocchi, M. Oostrom, and T. W. Wiestma (2010).Using dispersivity values to quantify the effects of pore-scale flow focusing on enhanced reaction along transverse mixing zone, *Adv. Water Res.*, *33*, 525–535.

G. Chiogna, O. A. Cirpka, P. Grathwohl, M. Rolle, Center for Applied Geoscience, University of Tübingen, Sigwartstrasse 10, D-72076 Tübingen, Germany. (gabriele.chiogna@student.uni-tuebingen.de; olaf.cirpka@uni-tuebingen.de; grathwohl@uni-tuebingen.de; massimo.rolle@uni-tuebingen.de)